Published in final edited form as:

Leuk Res. 2009 December ; 33(12): 1670–1677. doi:10.1016/j.leukres.2009.03.001.

OH-2, a hyperdiploid myeloma cell line without an *IGH* translocation, has a complex translocation juxtaposing *MYC* near *MAFB* and the *IGK* locus

Thea Kristin Våtsveen[a,b,*], **Erming Tian**[a], **Stine H. Kresse**[c], **Leonardo A. Meza-Zepeda**[c,d], **Ana Gabrea**[e], **Oleg Glebov**[e], **Hong Yan Dai**[b], **Anders Sundan**[a], **W. Michael Kuehl**[e], **Magne Børset**[a,f]

[a]Department of Cancer Research and Molecular Medicine, Faculty of Medicine, Norwegian University of Science and Technology, Trondheim, Norway

[b]Department of Pathology and Medical Genetics, St. Olavs University Hospital, Trondheim, Norway

[c]Department of Tumor Biology, Radiumhospitalet, Rikshospitalet, Oslo, Norway

[d]Norwegian Microarray Consortium1, Department of Molecular Biosciences, University of Oslo, Oslo, Norway

[e]Genetics Branch, National Cancer Institute, Bethesda, MD, USA

[f]Department of Immunology and Transfusion Medicine, St. Olavs University Hospital, Trondheim, Norway

Abstract

Multiple myeloma can be classified into hyperdiploid (HRD) (with 48–74 chromosomes) and nonhyperdiploid tumors (usually with immunoglobulin heavy chain translocations). The OH-2 human myeloma cell line (HMCL) retains the same HRD genotype as the primary tumor, with extra copies of chromosomes 3, 7, 15, 19, and 21. Both OH-2 and primary cells have a complex secondary translocation in which the *IGK* 3′ enhancer is inserted between *MYC* and *MAFB*, resulting in dysregulation of both oncogenes. OH-2 provides a unique example of an HMCL and the corresponding primary tumor that are shown to share the same HRD genotype.

Keywords

Hyperdiploid; Array CGH; FISH; *MYC*; *MAFB*; *IGK*

[*]Corresponding author at: Department of Cancer Research and Molecular Medicine, Faculty of Medicine, Norwegian University of Science and Technology, Olav Kyrres gt. 9, N-7489 Trondheim, Norway. Tel.: +47 73 59 86 60; fax: +47 73 59 88 01., thea.k.vatsveen@ntnu.no (T.K. Våtsveen).

Conflict of interest statement

None declared.

Appendix A. Supplementary data

Supplementary data associated with this article can be found, in the online version, at doi:10.1016/j.leukres.2009.03.001.

1. Introduction

Multiple myeloma (MM) is a neoplasm of long-lived bone marrow plasma cells [1]. Both MM and pre-malignant monoclonal gammopathy of undetermined significance (MGUS) can be separated into two groups that are distinguished by chromosome content [2,3]. Approximately 50% of tumors are hyperdiploid (HRD), and contain 48–74 chromosomes, typically with extra copies of at least four of eight odd-numbered chromosomes (3, 5, 7, 9, 11, 15, 19, and 21). The remaining tumors are non-hyperdiploid (NHRD), containing <48 and/or >74 chromosomes. These two groups are further distinguished by *IGH* translocations with five reciprocal partners (4p16, MMSET/FGFR3; 11q13, Cyclin D1; 6p21, Cyclin D3; 16q23, MAF; and 20q12, *MAFB)* that are present in about 70% of NHRD tumors but only about 15% of HRD tumors. It appears that recurrent *IGH* translocations and hyperdiploidy are primary events that occur early in pathogenesis. Secondary translocations, which include most *IGH* rearrangements not involving one of the five recurrent partners, most *IGL* and *IGK* rearrangements, and *MYC* rearrangements, appear to contribute equally to progression of both HRD and NHRD tumor [4].

Despite a low proliferation index, there is increased expression of one of the three CYCLIN D genes in virtually all MGUS and MM tumors, suggesting that this is a unifying and early oncogenic event. Primary translocations can directly dysregulate Cyclin D1 or Cyclin D3, or indirectly dysregulate Cyclin D2 (transcription target of maf proteins and unknown mechanism for *MMSET/FGFR3* translocation). The HRD tumors lacking a primary translocation mostly express increased levels of Cyclin D1 (~70%), Cyclin D1 + Cyclin D2 (~10%), or Cyclin D2 (~20%) compared to normal plasma cells [5].

In contrast to intramedullary MM tumors, most (~60%) extramedullary (EMM) tumors have one of the recurrent *IGH* translocations, and less than 10% are HRD [6,7]. Similarly, human myeloma cell lines (HMCL) are derived almost exclusively from EMM tumors, mostly are NHRD and usually have one of the recurrent *IGH* translocations (~75%), suggesting that intramedullary HRD tumors are less likely to develop into EMM tumors or HMCL [8]. There are no known examples of HMCL that have been shown to be derived from a primary tumor that has a HRD genotype and does not have a recurrent *IGH* translocation [9].

OH-2 is a stroma-independent HMCL derived from an EMM tumor that developed following treatment and progression of an intramedullary MM tumor [10]. Previously, it was reported that the OH-2 HMCL, which has a doubling time of about four days, is completely dependent on interleukin (IL)-6, and human serum for stromal cell independent growth in culture. In this paper we report that the OH2 HMCL retains the same HRD genotype as the EMM tumor cells. We also characterize its chromosomal composition, some genetic anomalies, and some of its growth characteristics.

2. Materials and methods

2.1. Cell line, OH-2

The HMCL OH-2 was established in 1991 at St. Olavs University Hospital from pleural fluid of an MM patient in terminal stage of the disease [10]. The cell line is cultured in

RPMI 1640 (Gibco, Paisley, UK) with L-glutamine (100 μg/ml) and gentamicine (20 μg/ml), supplemented with 10% human serum (AIT, St. Olavs University Hospital, Trondheim, Norway) and IL-6 2 ng/ml, in a humidified atmosphere containing 5% CO_2 at 37 °C.

2.2. Primary cells from the patient who gave rise to the OH-2 cell line

Cells from the pleural fluid of the patient who gave rise to the OH-2 cell line were separated by lymphoprep centrifugation and kept in RPMI 1640 with 10% DMSO and 30% fetal calf serum (FCS) in liquid nitrogen, frozen at the day of sampling. Cells were thawed, and RNA and DNA were isolated shortly after thawing. The cell suspension contained 90–95% pure plasma cells. These cells are further called primary OH-2 cells. An epon-embedded biopsy taken 10 months before the pleura fluid harvest was unfortunately not applicable for either DNA analysis or immunohistochemistry.

2.3. Other HMCLs and culture conditions

JJN-3 [11], ANBL-6 (gift from Dr. D. Jelinek, Mayo Clinic, Rochester, MN), RPMI-8226(from America Type Culture Collection, Rockville, MD) and INA-6(gift from Dr. M. Gramatzki, Erlangen, Germany) are maintained as previously described [12,13].

2.4. Fluorescence in situ hybridization (FISH)

Probes for FISH were made from bacterial artificial chromosome (BAC) clones containing the desirable genomic region covering loci 2p11, 4p16, 11q13, 14q32, 16q23, 20q12 and 22q11. In addition a break-apart probe for *IGK* was purchased from Dako (Dako Cytomation, Glostrup, Denmark). Supplementary Table A shows probe loci and clones. Probes for 4p16, 11q13, 14q32 and 16q23 were gifts from R. Fonseca, probes for 20q12 and *IGK* from M. Kuehl, the rest was purchased from Invitrogen. Whole chromosome paint (WCP) probes for chromosome 2, 14, 20 and 22 in aqua, and chromosome 8 in green (Applied Spectral Imaging, Micro System AB, Spånga, Sweden) were used to verify genes on their respective chromosomes. CEP 2 and CEP 8 SpectrumAqua were used to label the centromeric region in the chromosomes (Vysis, Abbot Laboratories, Des Plaines, IL). FISH with WCP and inlab LSI probes were used as follows: 2μl LSI probe in water + 2 μl WCP with 6 μl LSI hybridization buffer(Vysis).For *IGK*2μl WCP 2 and 8μl *IGK* probe mix(Dako) were used. Metaphase spreads were made according to the standard methods [14]. The metaphases were prepared at least 1-week prior to use without additional heating or chemical treatment. Method and microscopy was performed as described earlier [12].

2.5. Karyotyping

Conventional cytogenetic methods Giemsa-banding (G-banding) and spectral karyotyping (SKY) were performed after standard procedure as described [15].

2.6. Microarray-based comparative genomic hybridization (array CGH)

The genomic microarray was done using 500 ng genomic DNA sample from OH-2 cell line and primary cells after methods as described [16,17].

2.7. Southern blot for IGH, IGK and MAFB

Southern blots were performed on genomic DNA from OH-2 to look for *IGH* illegitimate switch recombination fragments, as previously described [18].

2.8. Gene expression profiling

Total RNA was profiled and analyzed as described previously (8,24), using Affymetrix HG-U133_Plus_2.0 Chips (Affymetrix, Santa Clara, CA). Profiling data were available for 559 newly diagnosed MM tumors (GEO accession GSE2658;http://www.ncbi.nlm.nih.gov) and 46 HMCL (http://www.broad.mit.edu/mmgp/pages/publicPortalHome.jsf). The expression of individual genes was normalized to the median expression of that gene in the entire sample set of 559 MM tumors and 47 HMCL. A MAF index (MAFI) was calculated from the median expression of 50 genes that are up-regulated in the MAF group [19], and the samples in Table 1 were arranged in descending order, based on the value of the MAFI. Other probe sets used in Table 1 included: CCND1, 208711_s_at; CCND2, 200951_s_at; CCND3, 201700_at; FGFR3, 204379_s_at; MMSET, 223472_at; MAF is the median of 206363_at; 209347_s_at; 209348_s_at; and 229327_s_at; *MAFB* is the median of 218559_s_at; and 222670_s_at; and *MYC* is 202431 _s_at. A proliferation expression index, P(12), was calculated from the median expression of twelve genes that are included in a proliferation signature [8].

2.9. Real-time RT-PCR on cyclin Ds, and MAFB

Total RNA from OH-2, INA-6 and ANBL-6 cells cultured as described, was isolated using RNeasy Mini Kit (Qiagen, Crawley, UK), with DNase treatment. cDNA was made from RNA using SuperScript®III First Strand Synthesis System for RT-PCR (Invitrogen). Cyclin D1-3 and *MAFB* TaqMan primers, (HS00765553.A1, HS00277041.A1, HS01017690_g1 and HS00271378_s1 respectively, TaqMan, Gene Expression Assays, Applied Biosystems, Foster City, CA), were used to detect cyclin Ds and *MAFB* expression. A control without reverse transcriptase added was used for the one exon gene *MAFB* to make sure there was no genomic DNA contamination. The comparative Ct-method was used for quantization with *GAPDH* (HS99999905_m1) as housekeeping gene.

2.10. Sequencing of TP53 and RAS

TP53, NRAS, HRAS or *KRAS2A/B* cDNA was PCR-amplified and sequenced to examine for nucleotide mutations. All RT-PCR reactions were purified with QIAquick PCR Purification Kit (Qiagen) and directly sequenced using BigDye Terminatorv1.1 Cycle Sequencing Kit (Applied Biosystems, Foster City, CA), DyeEx 2.0 Spin Kit (Qiagen) was used to purify the sequencing reaction that was analysed on ABI3100 Genetic Analyzer (Applied Biosystems). Details of primers and primer position are listed in Supplementary Figs. B and C.

3. Results

3.1. OH-2 does not have an IGH translocation

Using a split probe strategy on metaphase spreads, there was no dissociation of the centromeric and telomeric probes for the *IGH, IGK*, or *IGL* loci (Fig. 1a–c). OH-2 was also tested with dual fusion probes for the recurrent *IGH* translocation partner loci at 4p16,6p21, 11q13, 16q23, and 20q12, but no cryptic translocation involving *IGH* with any of these loci was detected (not shown). WCP probes confirmed that the *IGH, IGK*, and *IGL* loci were on chromosomes 14, 2, and 22, respectively. However, it was noted that there was a complex translocation near the *IGK* locus on chromosome 2, with both *IGK* probes localizing to der(2) (Fig. 1b). Southern blots identified 4.4 and 4.7 kb HindIII 5′ switch mu/3′ switch gamma legitimate switch recombination fragments, consistent with normal rearrangements involved in expression of IgG by the OH-2 tumor cells (not shown), but no illegitimate switch recombination fragments were detected.

3.2. Identical hyperdiploid chromosome content of OH-2 cell line and primary tumor

Conventional G-banding and SKY analyses (Fig. 2a and b) revealed the presence of 48–51 chromosomes, with trisomies of chromosomes 3, 7, 15, 19, and 21, in the OH-2 HMCL. In addition to aneuploidy, ten translocations and one large interstitial deletion were identified (Fig. 2a and b). Unfortunately, karyotypic analyses are not available for either the initial intramedullary MM tumor or the EMM tumor. Therefore, array CGH was performed to check for additional chromosomal aberrations in OH-2, and to compare the OH-2 HMCL and the EMM tumor. The OH-2 HMCL and OH-2 primary tumor showed virtually identical array CGH patterns apart from a 10q deletion and amplification of a portion of 8q that were uniquely present in the HMCL (Fig. 2c). Significantly, array CGH analyses confirmed in both the cell line and tumor the extra copies of the five odd-numbered chromosomes, and also chromosome 14, which were confirmed by additional FISH analyses (not shown). Finally, the array CGH and karyotypic analyses also verified loss of one copy of chromosome 13, as well as loss of 1p and gain of 1q sequences.

3.3. OH-2 cell line and primary tumor cells express a high level of MAFB RNA

The gene expression profile of the OH-2 cell line was determined using an Affymetrix HG-U133_Plus_2 chip, and compared to results that are available for 46 other HMCL. Selected results are shown in Table 1. Strikingly, the OH-2 HMCL expresses *MAFB* RNA at a level that is higher than the three HMCL (SACHI, EJM, SKMM-1) that have t(14;20) translocations. Consistent with the expression of high levels of *MAFB*, the OH-2 cells express extremely high levels of Cyclin D2 RNA, low levels of Cyclin D3 RNA, and very low levels of Cyclin D1 RNA. Real-time PCR assays confirmed that the OH-2 primary tumors cells also express high levels of *MAFB* and Cyclin D2 but low levels of Cyclin D1 RNA (Fig. 3). Significantly, the OH-2 HMCL has a *MAF* expression signature that places it among the 42 MM tumors and 14 other HMCL that express high levels of *MAF* or *MAFB* RNA (Table 1 and Section 2). In addition to Cyclin D2, some other apparent *MAF* targets with expression levels at least tenfold above the median of the tumors and cell lines include integrin beta7, *ARK5*, and *MRF-1*. Finally, the *MYC* RNA level in the OH-2 HMCL is in the highest quartile of the 47 HMCL (Table 1).

3.4. MAFB and MYC are juxtaposed by a complex translocation process involving IGK

In view of the high level of *MAFB* expression in OH-2, we suspected the translocations involving chromosomes 2, 8, and 20, as der(20)t(2;20)(p11;q12), der(8)t(8;20)(q24;q12)t(8;20)(q24;q12) or der(8)t(8;20)(q24;q12) and der(2)t(2;8)(p11;?q24) might be the cause. To determine if there is a rearrangement near *MAFB,* we performed FISH with a *MAFB* probe, as well as nearby centromeric and telomeric probes, in combination with WCP 2, 8, and 20, and also CEP probes for chromosomes 2 and 8 (Fig. 4c and e). *MAFB* is normally located at 20q11.2–q13.1 (http://www.genecards.org). There is one intact copy of chromosome 20 (Fig. 4b), but the *MAFB* locus was also translocated to chromosome 8. There were two clones of the HMCL, with either der(8)t(8;20)(q24;q12)t(8;20)(q24;q12) (~30%) or der(8)t(8;20)(q24;q12) (~70%), each paired with a normal chromosome 8. The translocated *MAFB* was localized at the 8;20 junction on der(8), or on both 8;20 junctions on der(8)t(8;20)t(8;20) (Fig. 4e and f). Probes that were about 400 and 700 kb centromeric to *MAFB* were present only on der(20), and a probe that was about 1100 kb telomeric to *MAFB* was present only on der(8) (Table 2). Thus the breakpoint on chromosome 20 apparently occurred less than 400 kb centromeric to *MAFB*. A *MYC* probe hybridized to the 8;20 junction on der(8) or to both 8;20 junctions on der(8)t(8;20)t(8;20),but not to der(2)t(2;8) (Fig. 4f and g). Therefore, *MYC* and *MAFB* are juxtaposed on both der(8). Despite the lack of a Vkappa/Ckappa split by conventional FISH analyses (Fig. 1b) we suspected that a Ckappa enhancer was juxtaposed to *MAF* and *MYC*. By using a relatively small BAC that included intronic and 3′ enhancer sequences from the *IGK* locus, we detected a hybridization signal on der (8)t(8;20)(q24;q12) (Table 2). A similar result was obtained with a pair of PCR probes that included 25 kb of sequences that encompass the intronic enhancer, the 3′ enhancer, and the 3′ kappa deleting element (Fig. 4d) (Table 2). The co-localization of one or both kappa enhancers together with *MYC* and *MAFB* was confirmed, and is present in all t(8;20) junctions (Fig. 4d). Interphase FISH analyses confirmed a *MAFB/MYC* fusion signal, both in the cell line and in primary tumor cells, thereby demonstrating that the close (<500 kb) juxtaposition of these two genes occurred in the patient (Fig. 4f and g). The complex der(8)t(8;20)t(8;20) was also present in the EMM tumor cells (Fig. 4f and g). These and additional FISH mapping studies are summarized in Table 2 and Fig. 4.

3.5. Mapping breakpoints near MAFB, MYC, and kappa enhancer by high density array CGH

The co-localization of *MAFB*, *MYC*, and kappa sequences on both kinds of der(8) suggested that breakpoints should be localized telomeric of *MYC*, on both sides of kappa sequences, and centromeric to *MAFB* (Fig. 5). The rearrangements involving chromosomes 2, 8, and 20 appeared to be balanced in most cells, but a partial imbalance was suggested by the duplication of the t(8;20) junction in about 30% of OH2 cells. Therefore, high density tiling CGH arrays were designed in an attempt to identify breakpoints near the *MAFB, MYC*, and kappa enhancer sequences. As a result of this analysis, we identified breakpoints, as manifested by an approximately 30% decrease in copy number, involving all three loci: 598 kb telomeric of *MYC*, 148 kb centromeric of *MAFB*; 18.6 kb telomeric and 9.9 kb centromeric of the 3′ kappa enhancer. These results (Supplementary Fig. D) indicate that the 3′ kappa enhancer effectively is inserted between the *MYC* and *MAF*genes, so that both

genes can be dysregulated by the same enhancer element. The combined FISH and array CGH results are consistent with sequential translocations as depicted in Fig. 5.

3.6. Additional genotypic and phenotypic characteristics of OH-2

The sequence of *KRAS* was normal, but there was a CAA (GLN) to AAA (LYS) mutation in codon 61 of *NRAS*. Although all but three (KMS-28BM; KMS-28PE; XG-6) of 46 HMCL either have a mutation in *TP53*, no or very low expression of *TP53*, or an increased level of *MDM-2* expression (M. Kuehl, unpublished), there were no sequence abnormalities of *TP53* or RNA expression abnormalities of *TP53* or *MDM-2* in OH-2. Similarly, although approximate 50% of the 46 HMCL have inactivated either p18/NK4c or *RB1* [20], the RNA expression of both of these genes appears to be normal in OH-2 (data not shown). Surprisingly, despite an extremely slow rate of growth in culture (below), the OH-2 HMCL has a proliferation expression index of 18.9, the fourth highest of the 47 HMCL.

4. Discussion

Approximately 50% of MM tumors are HRD and do not have one of the five recurrent *IGH* translocations. However, this genotype is found in less than 10% of reported EMM tumors [6,7]. It remains unclear to what extent this is due to a decreased probability that HRD tumors progress to an extramedullary phase versus a loss of the HRD genotype associated with this progression. Significantly, for the very limited composition of HRD EMM tumors that have been reported, it is unknown whether the corresponding intramedullary MM tumor had the same HRD genotype. Similar to EMM, from which virtually all HMCL are derived, HMCL only infrequently are HRD in the absence of one of the five recurrent *IGH* translocations [4,21]. For example, of the 46 HMCL (excluding OH-2) in Table 1, only ten (22%) do not have one of the recurrent *IGH* translocations. Five (10% overall) of these HMCL have a HRD chromosome content (RPMI 8226, 60 chromosomes; XG-2, 49 chromosomes; JK-6L, 50 chromosomes; KHM-1B, 59 chromosomes; OCI-MY1, 49 chromosomes). Unfortunately, it is not known whether or not the corresponding intramedullary MM tumor or EMM tumor had the same chromosome number as these five HMCL.

As summarized above, the OH-2 HMCL, which was derived from an EMM tumor, does not have an *IGH* translocation and retains the same HRD genotype as the extramedullary tumor, with extra copies of chromosomes 3, 7, 15, 19, and 21. This provides a unique example of an HMCL and the corresponding primary tumor that share the same HRD genotype. However it has a complex translocation involving the *IGH* locus, which is juxtaposed with both *MYC* and *MAFB*. The OH-2 HMCL and primary EMM tumor expresses very high levels of Cyclin D2 but only low levels of Cyclin D1, consistent with the genotype of the 20% of HRD MM tumors that express increased levels of Cyclin D2 but not Cyclin D1 [8]. The OH-2 HMCL is similar to the RPMI8226 HMCL in that both have dysregulated *MYC* through complex translocations events that juxtapose *MYC* with *MAFB* and IgK or MAF and IgL, respectively [4].

Other notable features of the OH-2 HMCL include the loss of 1p sequences, gain of 1q sequences, deletion of chromosome 13, and lack of trisomy 11, all of which are associated

with the poorest clinic outcome amongst the hyperdiploid patient group (Carrasco et al.). These genetic signatures correspond to the aggressive disease in the patient whose malignant cells generated the OH-2 cell line [10]. Despite an extremely high expression proliferation index and dysregulation of *MYC*, the OH-2 HMCL has a doubling time of at least four days when grown *in vitro*. In this regard, it may be relevant that OH-2 is one of the few HMCL that does not have a mutation or markedly decreased expression of *TP53* or a substantial increase in *MDM-2* expression. It is also worth noticing the gene expression profile study by Chng et al. that classified different clusters of hyperdiploid myeloma patients, where one of the clusters is defined by the overexpression of *PRL-3, SOCS, HGF* and *IL-6* genes [22]. We have recently published that PRL-3 is highly over-expressed in OH-2 [12]. Other experiments in our lab have shown that IL-6 induces transcription of *HGF* in OH-2 (Hov personal communication).

It is a pertinent question why it seems more difficult to establish HMCL from tumors that are HRD and lack one of the five recurrent *IGH* translocations. A reasonable answer could be that tumors with this genotype are more dependent on the microenvironment than cells with primary *IGH* translocations. The strict dependence of OH-2 on mitogenic cytokines and on human serum supports this. In addition it is worth noticing that OH-2 grows significantly slower than the other HMCLs in our lab. In our experience, other IL-6-dependent cell lines become IL-6-independent after culture for extended periods, but we have never experienced this with OH-2. Most HMCLs reported in the literature grow in medium supplemented with FCS, but OH-2 cells are impossible to wean from their dependence on human serum, which is something that remains to be clarified. Anyway, one way of circumventing the problem with establishing similar cell lines might be to use human serum in the growth medium. An additional genetic answer to this might be the acquisition of autonomous Cyclin D dysregulation. In fact, it is remarkable that all of the six HRD HMCL (above) express high levels of Cyclin D2, whereas ~70% of HRD MM tumors express increased levels of Cyclin D1 (but not of Cyclin D2) compared to normal bone marrow plasma cells [8]. Significantly, of two recently reported stromal cell dependent HMCL, generated from HRD primary tumors, neither expresses Cyclin D1; instead, one expresses high levels of Cyclin D2 and the other expresses extremely low levels of *RB1*, perhaps eliminating the need for increased expression of a Cyclin D gene [23]. One possible explanation is that HRD MM tumors, and especially those that ectopically express Cyclin D1, are dependent on signals from the bone marrow microenvironment to enable biallelic expression of a Cyclin D gene. If this is true, then progression to independence from the bone marrow microenvironment might require an alternative mechanism to dysregulate a Cyclin D gene. Perhaps OH-2, and also RPMI 8226 and XG-2, have accomplished this by virtue of a genomic rearrangement that dysregulates *MAF* or *MAFB*, both of which increase expression of Cyclin D2.

Supplementary Material

Refer to Web version on PubMed Central for supplementary material.

Acknowledgements

We thank Ola Myklebost at the Radiumhospitalet, Rikshospitalet/NMC for access to the microarray platform. We also thank Berit Størdal for taking good care of the cell lines.

This work was supported by the Norwegian Research Council (Grant 170637/V40), Familien Blix' Fond, Rakel og Otto Bruuns legat and the University of Oslo (EMBIO), and also by the Intramural Research Program of the NIH, National Cancer Institute, Center for Cancer Research (W.M.K.). The genomic microarrays were provided by the Norwegian Microarray Consortium (NMC) at the national technology platform, and supported by the functional genomics programme (FUGE) in the Research Council of Norway.

References

[1]. Chng WJ, Glebov O, Bergsagel PL, Kuehl WM. Genetic events in the pathogenesis of multiple myeloma. Best Pract Res Clin Haematol 2007;20(12 (4)):571–96. [PubMed: 18070707]

[2]. Fonseca R, Debes-Marun CS, Picken EB, Dewald GW, Bryant SC, Winkler JM, et al. The recurrent IgH translocations are highly associated with nonhyperdiploid variant multiple myeloma. Blood 2003;102(10(7)):2562–7. [PubMed: 12805059]

[3]. Smadja NV, Bastard C, Brigaudeau C, Leroux D, Fruchart C. Hypodiploidy is a major prognostic factor in multiple myeloma. Blood 2001;98(10 (7)):2229–38. [PubMed: 11568011]

[4]. Gabrea A, Martelli ML, Qi Y, Roschke A, Barlogie B, Shaughnessy JD Jr, et al. Secondary genomic rearrangements involving immunoglobulin or MYC loci show similar prevalences in hyperdiploid and nonhyperdiploid myeloma tumors. Genes Chromosome Cancer 2008 7;47(7): 573–90.

[5]. Bergsagel PL, Kuehl WM. Molecular pathogenesis and a consequent classification of multiple myeloma.J Clin Oncol 2005;23(9 (26)):6333–8. [PubMed: 16155016]

[6]. Avet-Loiseau H, Daviet A, Brigaudeau C, Callet-Bauchu E, Terre C, Lafage-Pochitaloff M, et al. Cytogenetic, interphase, and multicolor fluorescence in situ hybridization analyses in primary plasma cell leukemia: a study of 40 patients at diagnosis. Blood 2001;97(2 (3)):822–5. [PubMed: 11157506]

[7]. Tiedemann RE, Gonzalez-Paz N, Kyle RA, Santana-Davila R, Price-Troska T, Van Wier SA, et al. Genetic aberrations and survival in plasma cell leukemia. Leukemia 2008;22(5):1044–52. [PubMed: 18216867]

[8]. Bergsagel PL, Kuehl WM, Zhan F, Sawyer J, Barlogie B, Shaughnessy J Jr. Cyclin D dysregulation: an early and unifying pathogenic event in multiple myeloma. Blood 2005;106(7 (1)):296–303. [PubMed: 15755896]

[9]. Chng WJ, Fonseca R. Cell lines of hyperdiploid myeloma, are we there yet? Br J Haematol 2008;140(5):579–80. [PubMed: 18028478]

[10]. Borset M, Waage A, Brekke OL, Helseth E. TNF and IL-6 are potent growth factors for OH-2, a novel human myeloma cell line. Eur J Haematol 1994;53(7 (1)):31–7. [PubMed: 8062895]

[11]. Jackson N, Lowe J, Ball J, Bromidge E, Ling NR, Larkins S, et al. Two new IgA1- kappa plasma cell leukaemia cell lines (JJN-1 & JJN-2) which proliferate in response to B cell stimulatory factor 2. Clin Exp Immunol 1989;75(1 (1)):93–9. [PubMed: 2495201]

[12]. Fagerli UM, Holt RU, Holien T, Vaatsveen TK, Zhan F, Egeberg KW, et al. Overexpression and involvement in migration by the metastasis-associated phosphatase PRL-3 in human myeloma cells. Blood 2008;111(1 (2)):806–15. [PubMed: 17934070]

[13]. Ro TB, Holt RU, Brenne AT, Hjorth-Hansen H, Waage A, Hjertner O, et al. Bone morphogenetic protein-5, -6 and -7 inhibit growth and induce apoptosis in human myeloma cells. Oncogene 2004;23(4(17)):3024–32. [PubMed: 14691444]

[14]. Sawyer JR, Roloson GJ, Bell JM, Thomas JR, Teo C, Chadduck WM. Telomeric associations in the progression of chromosome aberrations in pediatric solid tumors. Cancer Genet Cytogenet 1996;90(8(1)):1–13. [PubMed: 8780739]

[15]. Sawyer JR, Lukacs JL, Thomas EL, Swanson CM, Goosen LS, Sammartino G, et al. Multicolour spectral karyotyping identifies new translocations and a recurring pathway for chromosome loss in multiple myeloma. Br J Haematol 2001;112(1 (1)):167–74. [PubMed: 11167798]

[16]. Meza-Zepeda LA, Kresse SH, Barragan-Polania AH, Bjerkehagen B, Ohnstad HO, Namlos HM, et al. Array comparative genomic hybridization reveals distinct DNA copy number differences between gastrointestinal stromal tumors and leiomyosarcomas. Cancer Res 2006;66(9(18)): 8984–93. [PubMed: 16982739]

[17]. Wang J, Meza-Zepeda LA, Kresse SH, Myklebost O. M-CGH: analysing microarray-based CGH experiments. BMC Bioinformatics 2004;6 (5): 74. [PubMed: 15189572]

[18]. Bergsagel PL, Chesi M, Nardini E, Brents LA, Kirby SL, Kuehl WM. Promiscuous translocations into immunoglobulin heavy chain switch regions in multiple myeloma. Proc Natl Acad Sci USA 1996 11 26;93(24):13931–6. [PubMed: 8943038]

[19]. Zhan F, Huang Y, Colla S, Stewart JP, Hanamura I, Gupta S, et al. The molecular classification of multiple myeloma. Blood 2006;108(9 (6)): 2020–8. [PubMed: 16728703]

[20]. Dib A, Peterson TR, Raducha-Grace L, Zingone A, Zhan F, Hanamura I, et al. Paradoxical expression of INK4c in proliferative multiple myeloma tumors: biallelic deletion vs increased expression. Cell Div 2006;1:23. [PubMed: 17049078]

[21]. Drexler HG, Matsuo Y. Malignant hematopoietic cell lines: in vitro models for the study of multiple myeloma and plasma cell leukemia. Leuk Res 2000;24(8 (8)):681–703. [PubMed: 10936422]

[22]. Chng WJ, Kumar S, Vanwier S, Ahmann G, Price-Troska T, Henderson K, et al. Molecular dissection of hyperdiploid multiple myeloma by gene expression profiling. Cancer Res 2007;67(4 (7)):2982–9. [PubMed: 17409404]

[23]. Li X, Pennisi A, Zhan F, Sawyer JR, Shaughnessy JD, Yaccoby S. Establishment and exploitation of hyperdiploid and non-hyperdiploid human myeloma cell lines. Br J Haematol 2007;138(9 (6)): 802–11. [PubMed: 17760811]

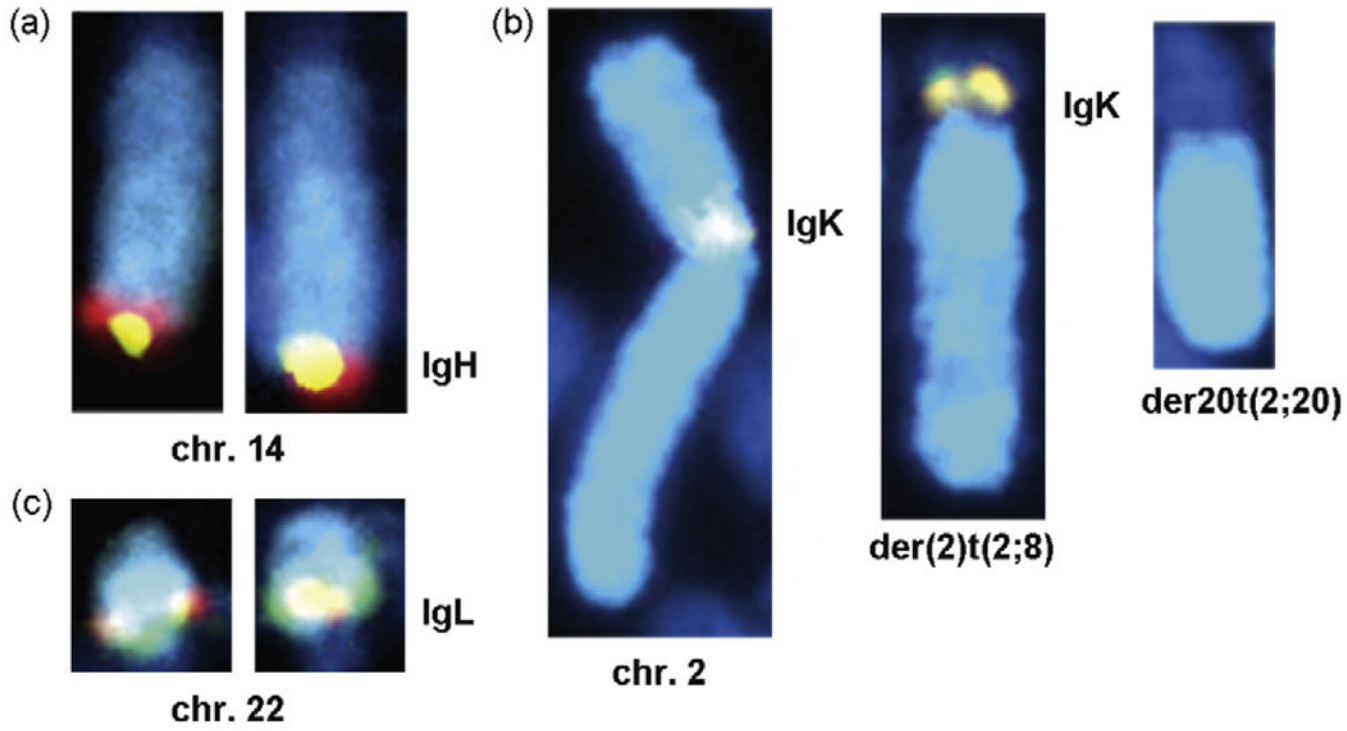

Fig. 1.

FISH detects intact immunoglobulin genes. (a)–(c) Break-apart probes for *IGH, IGK* and *IGL,* (a)–(c) respectively, were used together with WCP for the corresponding chromosome 14, 2 and 22. The yellow co-localization signal for the immunoglobulin loci indicates co-localization of the probes. (a)WCP 14 and *IGH* break-apart probe show no abnormalities. (b) WCP 2 and *IGK* break-apart probe suggest no translocation within the *IGK* locus. On the two derivatives involving chromosome 2, both *IGK* probes remain together near the breakpoint on der(2) (Fig. 2b). (c) WCP 22 and *IGL* break-apart probe show no abnormalities (original magnification: 1000×).

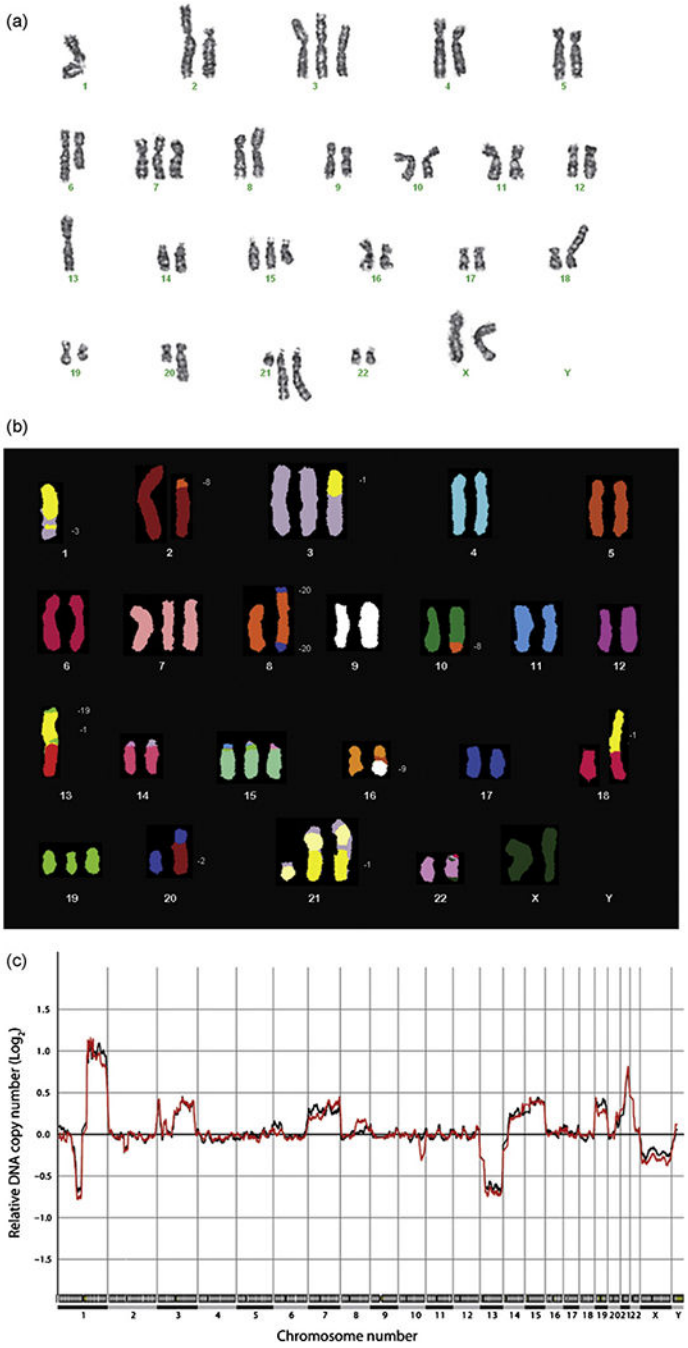

Fig. 2.

The karyotype of OH-2 has a hyperdiploid profile. (a) Representative G-band with karyotype; 48–51 ⟨2n⟩,XX,−1, der(1)t(1;3)(q12;q13)del(3)(q24), der(2)t(2;8)(p11;?), +3, der(3)t(1;3)(p22;q21), del(6)(q23), +7, der(8)t(8;20)(q24;?q12)t(8;20)(q24;?q12), der(10)t(8;10)(?;q26), −13, der(13)(13qter→13p11::1q21→1q41::19?p13), +15, der(16)t(9;16)(?;?), der(18)t(1;18)(q21;p11), der(20)t(2;20)(p11;q13), +21, der(21)t(1;21)(q21;q22)dup(1)(q21q32)x2. (b) SKY of the OH-2 cell line. The G-band and the SKY analyses demonstrate the aberrations in the OH-2 cell line. The chromosome number and the

trisomy 3, 7, 15, 19 and 21 indicate a hyperdiploid karyotype. (c) Array CGH shows the genomic aberrations of the OH-2 primary cells (black) and the OH-2 cell line (red) in the same plot. Log_2 ratios for each of the BACs and PACs are plotted according to chromosome position. Log_2 values ~0.6 indicate one extra copy of the chromosome area, and values ~−1 indicate loss of one copy of the chromosome area. Smoothing of the mean of 15 clones is used in this plot. Detailed array CGH in supplementary Fig A.

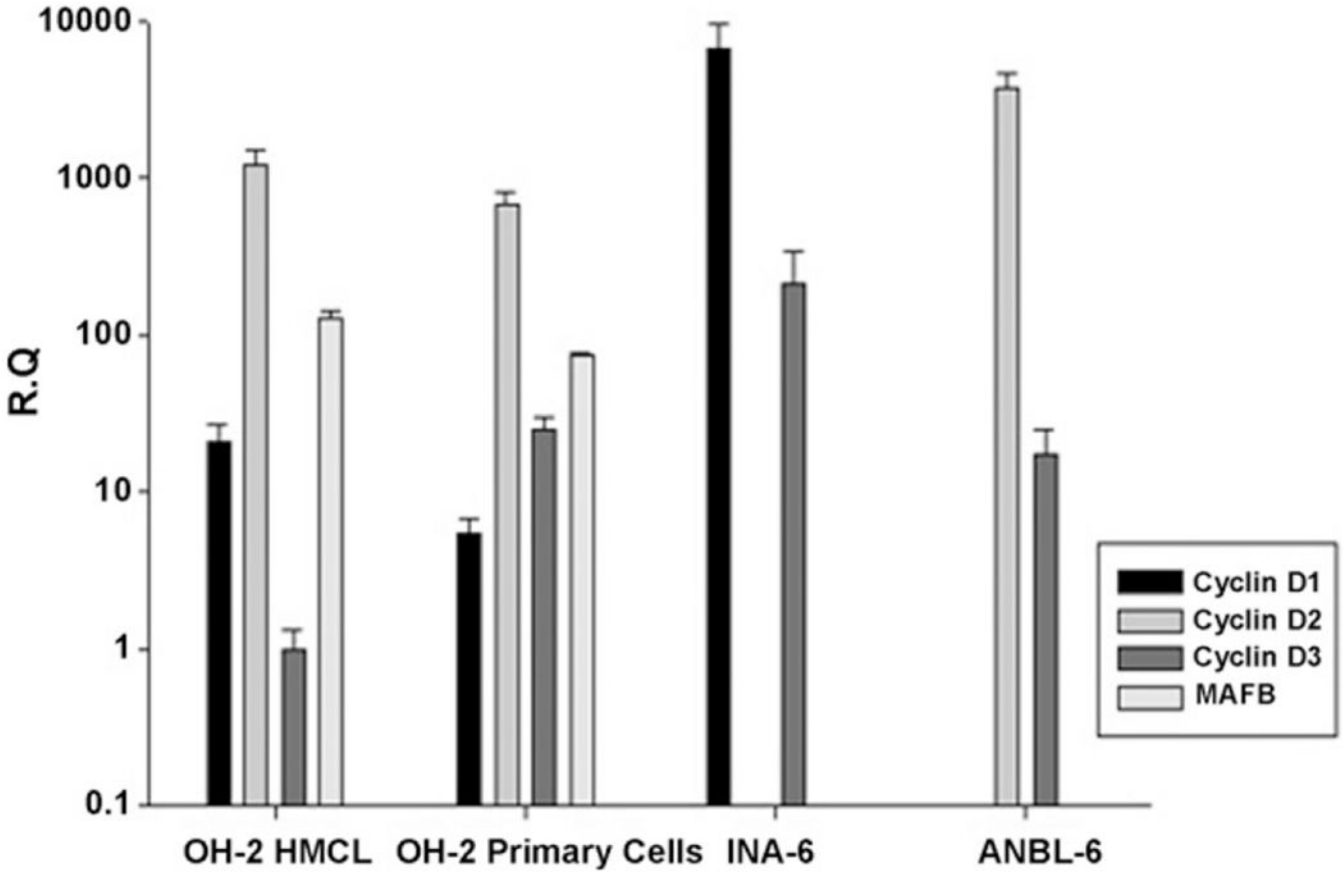

Fig. 3.

Expression of *CCNDs* and *MAFB* mRNA in primary and HMCL OH-2. The expression patterns of OH-2 primary cells and OH-2 cell line are quite similar. Both have high expression of cyclin D2 and low expression of cyclins D1 and D3, but with a higher expression of cyclin D3 in the primary sample. INA-6 is a t(11;14) cell line and expresses high amounts of cyclin D1. ANBL-6 is a t(14;16) cell line and expresses high amounts of cyclin D2. *MAFB* is almost equally expressed in HMCL and primary OH-2 cells. The scale is in log10 and the values are relative quantitation based on the delta Ct method (see Section 2). Cyclin D3 expression in OH-2 cell line was set as 1 and all values are normalized to this. Error bars show standard deviation of triplicates.

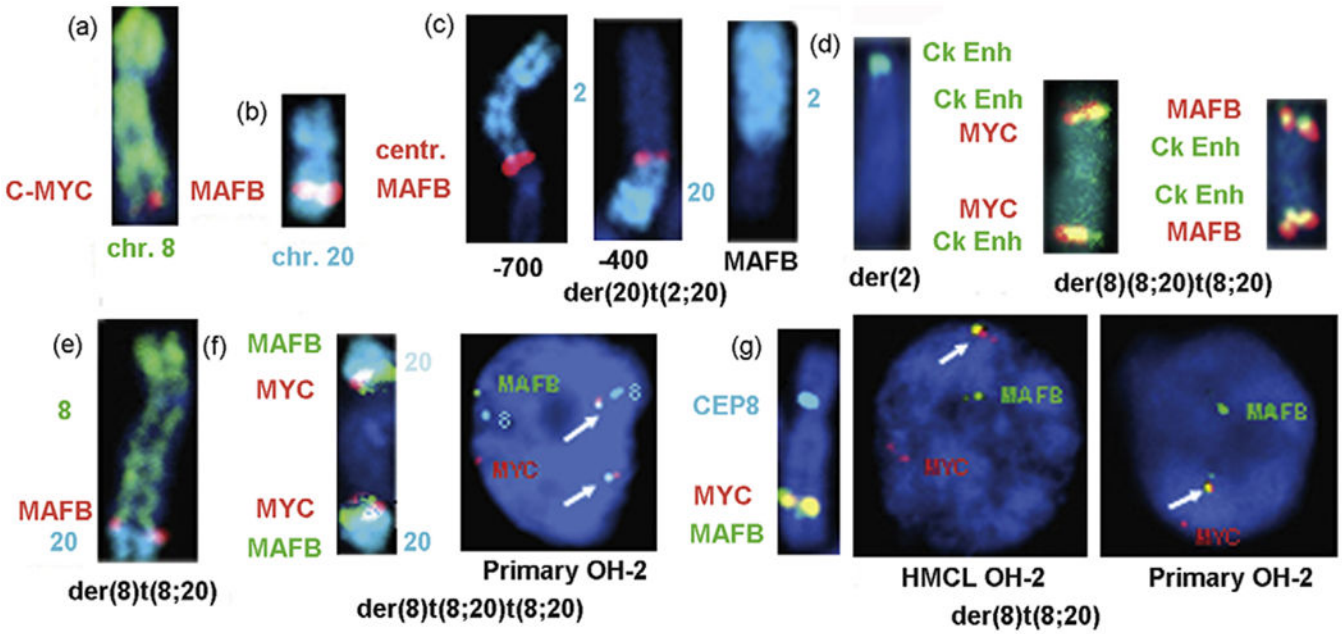

Fig. 4.

MAFB and *MYC* is juxtaposed in a complexed translocation. (a) Normal chromosome 8 with WCP8 in green and *MYC* red; (b) normal chromosome 20 with WCP20 in aqua and *MAFB* red; (c) *MAFB* and probes centromeric to *MAFB* localize the breakpoint on der(20); (d) Ck Enh is a PCR derived probe covering the enhancers in *IGK,* co-localizes with *MAFB* and *MYC* on both junctions on der(8); (e) der(8)t(8;20) with *MAFB* red; (f) der(8) is replaced by der(8)t(8;20)t(8;20) in some cells, with *MYC* and *MAFB* juxtaposed at both 8;20 junctions. This is also detected in primary OH-2 cells giving two fusion *MYC/MAFB* (arrows) signals together with two CEP8 and one normal *MYC* and *MAFB* signals; (g) most of the cells have only one 8;20 junction. This is also detected in interphase nuclei with *MYC/MAFB* (arrow) fusion signal both in the HMCL and primary cells.

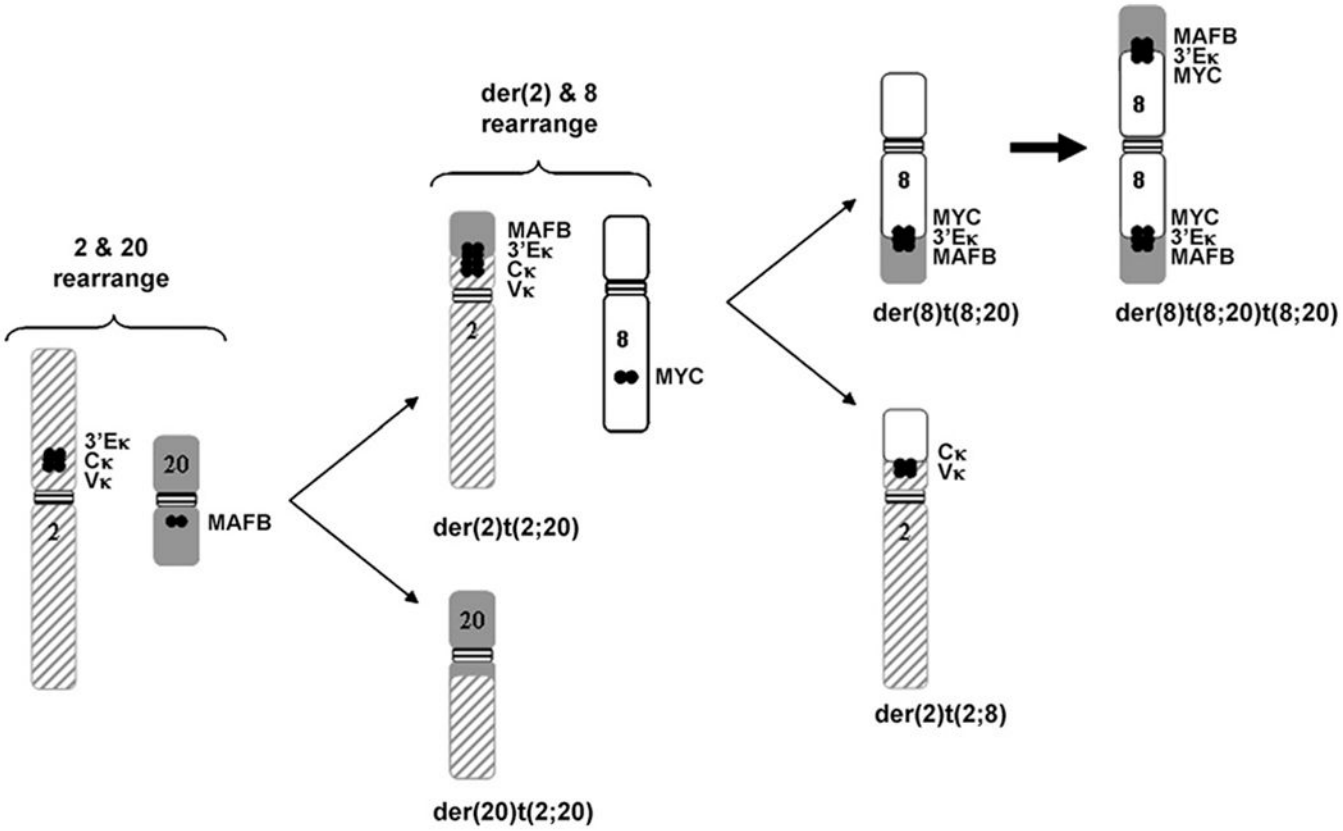

Fig. 5.

How did the complex translocation process occur? There might have been an initial reciprocal translocation between chromosomes 2 and 20, which juxtaposed *MAFB* and the *IGK* locus on der(2), but without the usual split between the two *IGK* probes. A subsequent reciprocal translocation between der(2) and normal chromosome 8 would have generated der(8)t(8;20) and der(2)t(2;8), with the *IGK* sequences localized on der(2), but with co-localization of *MYC*, *MAFB*, and *IGK* enhancer sequences on der(8). The der(8)t(8;20)t(8;20) must have been generated subsequently by a rearrangement of der(8) that included duplication of the 8;20 junction. See Table 2 and text for further details.

Leuk Res. Author manuscript; available in PMC 2020 January 06.

Table 1

Selected HG-U133-Plus-2 expression results in 47 myeloma cell lines. The values are normalized for 606 samples, including 559 untreated MM tumors and 47 HMCL. The sample order is in descending order based on a MAF index (MAFI), with 15 HMCL and 42 of 45 MM tumors in the MF group (not shown) included among the 57 samples with the highest MAF index. Translocation (TLC) targets are mainly associated with *IGH* but a few involve *IGL* (*), *IGK* (§) or no detectable Ig sequences (#). $ All HMCL express *MYC* except for PE-2 and U266, which express *MYCN* and *MYCL*, respectively (MK, unpublished). See Section 2 for additional details.

HMCL	TLC targets	MAFI	CCND1	CCND2	CCND3	FGFR3	MMSET	MAF	MAFB	MYC$
MM.1S	MAF	9	0.0	25.3	2.3	0.9	5.1	91.5	0.9	7.8
ANBL6	MAF	27	0.4	26.2	0.9	1.0	0.2	29.8	0.3	0.7
8226	MAF*	29	0.7	8.7	1.0	0.6	1.8	63.5	0.6	7.5
OH-2	MAFB§	30	0.5	30.9	1.7	0.8	2.1	7.6	139.4	4.8
XG-6	MAF*	39	0.3	12.0	1.7	1.5	1.8	10.1	0.4	11.0
JJN-3	MAF	41	0.3	6.0	0.9	0.9	4.0	37.3	0.2	4.5
SACHI	MAFB	42	0.5	6.5	0.8	0.9	1.7	1.0	118.3	4.7
ARP-1	MAF	43	0.1	10.7	1.7	0.9	3.0	12.7	0.4	3.0
KMS-26	MMSET	45	0.2	8.4	1.4	214.2	50.5	16.3	0.4	1.7
KMS-11	MMSET + MAF	46	0.3	7.8	0.6	713.0	17.0	14.6	0.7	1.1
OCI-MY5	MAF	47	0.5	26.5	0.5	1.1	1.2	12.0	0.6	0.6
KMS-34	MMSET	48	0.1	21.2	0.8	214.6	18.2	13.0	2.2	5.3
SKMM-1	MAFB	53	0.1	21.8	0.8	1.0	4.2	2.3	23.7	3.6
H929	MMSET	55	1.1	23.5	1.9	194.1	21.5	10.5	1.3	0.8
EJM	MAFB	56	0.5	25.1	1.0	2.5	1.8	0.7	79.6	2.7
LP1	MMSET	64	0.1	28.9	1.3	33.6	6.1	13.4	1.9	2.7
KMS-20		67	0.4	27.4	0.8	1.5	8.7	0.3	0.4	7.5
KMM-1	CCND3	89	0.3	22.3	15.6	5.7	2.1	4.8	0.5	3.5
Delta-47		113	0.3	20.8	1.3	0.6	2.8	0.2	0.5	5.3
OCI-MY7	CCND1	119	5.4	0.1	1.8	0.9	3.2	0.2	0.6	4.3
JK6L		144	0.2	15.0	0.9	1.1	4.2	1.8	0.3	4.4
XG-7	MMSET	146	0.4	7.1	1.7	2.1	9.7	5.6	0.7	1.8
MM-M1	CCND1	160	13.8	4.7	1.2	1.1	1.8	0.3	0.5	5.1
KARPAS-620	CCND1	173	5.9	1.0	2.0	8.8	1.3	0.2	0.4	1.7

HMCL	TLC targets	MAFI	CCND1	CCND2	CCND3	FGFR3	MMSET	MAF	MAFB	MYC$
KMS-28PE	MMSET	174	0.3	0.1	2.5	1021.0	11.3	0.1	0.9	2.0
OPM-1	MMSET	191	0.3	7.4	1.0	248.4	14.2	3.9	2.1	0.7
UTMC-2	MMSET	192	0.3	2.6	2.1	25.5	29.0	4.5	0.5	1.7
JIM-3	MMSET	196	0.1	12.1	4.3	0.8	12.8	7.1	0.4	1.6
OPM-2	MMSET	213	0.2	8.1	1.2	71.0	15.0	10.6	8.5	0.4
KMS-12BM	CCND1	217	11.3	0.0	0.7	0.8	2.0	0.2	0.4	6.1
L363	MAFB#	222	0.6	15.1	1.3	2.0	2.7	0.7	13.5	1.8
KMS-28BM	MMSET	228	0.1	0.1	5.3	690.0	11.4	0.3	0.5	1.8
KHM-11	MMSET	251	1.8	26.5	1.8	32.3	23.8	4.0	0.4	1.9
KHM-1B		252	0.4	2.8	0.7	0.8	1.1	0.8	0.5	2.0
INA-6	CCND1	277	6.4	0.1	1.2	0.9	0.7	0.7	0.4	2.4
KMS-18	MMSET	285	0.1	3.3	1.1	927.6	5.8	0.7	0.5	1.5
FR4		294	0.1	15.1	3.7	0.9	1.5	0.7	0.1	0.6
PE-2	MMSET	297	0.1	7.1	1.4	1.9	86.2	4.2	0.3	0.0
KMS-12PE	CCND1	307	5.0	0.1	1.8	1.3	5.8	0.4	0.3	4.8
U266	CCND1	328	6.5	2.1	0.6	8.9	0.7	0.2	0.6	0.0
XG-2	MAFB*	357	0.1	24.6	0.8	0.8	2.1	0.2	30.3	1.4
FLAM-76	CCND1	384	9.1	0.1	0.8	1.4	3.4	0.4	0.3	1.3
OCI-MY1		392	0.8	8.1	1.2	2.0	1.0	1.1	0.2	0.9
PE-1	CCND1	424	26.5	0.1	1.3	1.7	3.3	0.6	0.4	0.1
XG-1	CCND1	436	8.6	0.2	0.5	6.0	3.7	0.4	0.2	0.7
SKMM-2	CCND1	554	8.3	0.1	1.3	2.4	1.1	0.9	0.3	4.3
H1112	CCND1	588	10.4	0.1	0.9	1.1	5.2	0.1	0.3	0.3

The shaded entries in figure 1 are to be able to see the OH-2 cells easier. The darker shading to be able to assess the gene that are upregulated because of the primary translocation in the cell lines.

Leuk Res. Author manuscript; available in PMC 2020 January 06.

Table 2

FISH-mapping of translocated chromosomes. The positions of probes relative to the *IGK* constant region and the 5′ ends of the *MYC* and *MAFB* genes are indicated in kb, with negative values indicating a location 5′ of the gene.

	Gene/locus											
	IgK(V)	IgK	IgK[a]	IgK[a]	IgK	IgK	MYC	MAFB	MAFB	MAFB	MAFB	MAFB
Chromosome/probe	**−1021>−965**	**−146>+17**	**−1>+25**	**−4> +90**	**−45>+132**	**+132>+259**	**MYC**	**−1084>−972**	**−798>−613**	**−400>?**	**−92>+53**	**+1185>+1291**
der(20)t(2;20)(p11;q12)	0	0	0	0	+	+	0	+	+	+	0	0
der(8)t(8;20)(q24;q12)	0	0	+	+	0	0	+	0	0	0	+	+
der(8)t(8;20)(q24;q12)t(8;20)(q24;q12)	0	0	+	+	0	0	+	0	0	0	+	+
der(2)t(2;8)(p11;?q24)	+	+	+	+	+	0	0	0	0	0	0	0
der(10)t(8;10)(?;?q26)	0	0	0	0	0	0	0	0	0	0	0	0

[a]These smaller PCR (−1>+25 kb) and BAC probes that were labeled with biotin and reacted with FITC-streptavidin uniquely detected *IGK* sequences at 8;20 junctions on both kinds of der(8).